

# One-pot preparation and applications of self-healing, self-adhesive PAA-PDMS elastomers

Yujin Yao<sup>1</sup>, Huiling Tai<sup>1, †</sup>, Dongsheng Wang<sup>1, 2, †</sup>, Yadong Jiang<sup>1</sup>, Zhen Yuan<sup>1</sup>, and Yonghao Zheng<sup>1</sup>

<sup>1</sup>State Key Laboratory of Electronic Thin Films and Integrated Devices, School of Optoelectronic Science and Engineering, University of Electronic Science and Technology of China, Chengdu 610054, China

<sup>2</sup>State Key Laboratory of Polymer Materials Engineering, Sichuan University, Chengdu 610065, China

**Abstract:** A new family of transparent, biocompatible, self-adhesive, and self-healing elastomer has been developed by a convenient and efficient one-pot reaction between poly(acrylic acid) (PAA) and hydroxyl-terminated polydimethylsiloxane (PDMS-OH). The condensation reaction between PAA and PDMS-OH has been confirmed by attenuated total reflection Fourier transform infrared (ATR-FTIR) spectra. The prepared PAA-PDMS elastomers possess robust mechanical strength and strong adhesiveness to human skin, and they have fast self-healing ability at room temperature (in ~10 s with the efficiency of 98%). Specifically, strain sensors were fabricated by assembling PAA-PDMS as packaging layers and polyetherimide-reduced graphene oxide (PEI-rGO) as strain-sensing layers. The PAA-PDMS/PEI-rGO sensors are stably and reliably responsive to slight physical deformations, and they can be attached onto skin directly to monitor the body's motions. Meanwhile, strain sensors can self-heal quickly and completely, and they can be reused for the motion detecting after shallowly scratching the surface. This work provides new opportunities to manufacture high performance self-adhesive and self-healing materials.

**Key words:** self-healing; PDMS elastomer; self-adhesiveness; condensation reaction

**Citation:** Y J Yao, H L Tai, D S Wang, Y D Jiang, Z Yuan, and Y H Zheng, One-pot preparation and applications of self-healing, self-adhesive PAA-PDMS elastomers[J]. *J. Semicond.*, 2019, 40(11), 112602. <http://doi.org/10.1088/1674-4926/40/11/112602>

## 1. Introduction

A self-healing material is a functional material that mimics the self-healing capability of natural biomaterials, which extend the lifetime, enhance the durability and increase the reliability of these materials<sup>[1–5]</sup>. Self-healing materials have been extensively investigated in a wide range of applications, including sensors<sup>[6–10]</sup>, smart materials<sup>[11, 12]</sup> and medical diagnosis<sup>[13–17]</sup>, energy storage<sup>[18, 19]</sup>, self-powered device<sup>[20]</sup>, etc. Recently, research of self-healing materials has mainly focused on hydrogels<sup>[21–25]</sup> and elastomers<sup>[26, 27]</sup>. Hydrogels with high water content can self-heal quickly under room temperature without any external stimulus. However, the poor mechanical properties and long-term stability of hydrogels limit their applications. In contrast, elastomers have prominent advantages in practical applications due to their excellent elasticity and stability.

Self-healing elastomers can be fabricated by incorporating dynamic bonding (e.g. hydrogen bonds<sup>[28, 29]</sup>, coordinate bonds<sup>[30, 31]</sup>,  $\pi$ - $\pi$  stacking<sup>[32]</sup>, host-guest interaction<sup>[33–36]</sup>). Some of them can only self-heal triggered by external stimuli. For instance, Deng *et al.* reported a polydimethylsiloxane (PDMS) elastomer based on acylhydrazone groups, and its self-healing process was induced by treating with acetic acid or annealing at 120 °C<sup>[28]</sup>. Zhang *et al.* successfully prepared a nanostructured supramolecular elastomer with a dual non-covalent network of hydrogen bonding and metal-ligand co-

ordination<sup>[36]</sup>, which can self-heal quickly (~30 s) and spontaneously at room temperature. However, when applies in wearable devices, additional adhesive tapes were needed to immobilize the devices on skin, which was unfavorable to the sensitivity and comfortableness. Therefore, it is necessary and remains a challenge to design elastomers that simultaneously possess excellent self-healing ability, self-adhesiveness, and mechanical properties.

In this research, a novel transparent, self-healing and self-adhesive elastomer was fabricated by cross-linking poly(acrylic acid) (PAA) and hydroxyl-terminated polydimethylsiloxane (PDMS-OH) through a convenient and efficient one-pot reaction. The PAA-PDMS elastomers showed robust mechanical properties, self-adhesiveness, fast self-healing (within ~10 s) at room temperature and excellent self-healing efficiency (98%). Furthermore, strain sensors were fabricated by assembling PAA-PDMS elastomers as packaging layers and polyetherimide-reduced graphene oxide (PEI-rGO) as strain-sensing layers<sup>[37]</sup>. The PAA-PDMS/PEI-rGO sensors are mechanically stable, highly sensitive, self-adhesive, and they are biocompatible with skin. The self-healing process of PAA-PDMS/PEI-rGO sensors was extremely fast at room temperature without any external stimulus, and the healed sensors were able to detect slight physical deformations after starching on the surface.

## 2. Experimental

### 2.1. Materials

Hydroxyl-terminated polydimethylsiloxane (PDMS-OH, viscosity 2550–3570 cSt), N, N'-dicyclohexylcarbodiimide (DCC, 99%), 4-(dimethylamino) pyridine (DMAP,  $\geq$  99%) and

Correspondence to: H L Tai, [taitai1980@uestc.edu.cn](mailto:taitai1980@uestc.edu.cn); D S Wang, [wangds@uestc.edu.cn](mailto:wangds@uestc.edu.cn)

Received 16 APRIL 2019; Revised 27 MAY 2019.

©2019 Chinese Institute of Electronics

branched polyetherimide aqueous solution (PEI, 50% (w/v)) were purchased from Sigma-Aldrich. Poly(acrylic acid) (PAA,  $M_w \sim 450,000$ ) and Tetrahydrofuran (THF, AR, 99%) were purchased from Shanghai Aladdin Bio-Chem Technology Co, Ltd. Graphene oxide (GO) aqueous dispersion (2 mg/mL) was provided by Sinocarbon Materials Technology Co, Ltd. The GO aqueous dispersion (2 mg/mL) was diluted to 0.5 mg/mL, and the branched PEI aqueous solution (50% (w/v)) was diluted to 1% (w/v). All of the chemical reagents mentioned at this work were of analytical grades and used without further purification.

## 2.2. Preparation of PAA-PDMS elastomer

DCC (20 mg) and DMAP (5 mg) were dissolved in 40 mL THF. PAA (0.50 g) was then added to the mixture and stirred at 40 °C for 3 h. After slowly adding various amounts of PDMS-OH, the mixture was stirred continuously at 40 °C for 24 h to obtain a homogeneous solution. The mixture was heated at 90 °C for 20 min to remove the solvent, followed by spin-coating on glass substrate to prepare the PAA-PDMS films. Different PAA-PDMS films were prepared by varying the weight ratios between PAA and PDMS.

## 2.3. Fabrication of PAA-PDMS/PEI-rGO strain sensors

The PAA-PDMS/PEI-rGO strain sensors were prepared according to our previous work<sup>[37]</sup>. First, PEI-rGO composite films were treated with layer-by-layer self-assembly by alternately dipping 1% (w/v) PEI solution and 0.5 mg/mL GO dispersion. To control the initial resistance, the assembling time, thermal reduction time and temperature were strictly controlled. Subsequently, PAA-PDMS composite was spin-coated (600 rpm, 8 s) on the glass substrate with PEI-rGO composite film at room temperature. Finally, the PAA-PDMS elastomers were mechanically peeled from the glass, and coated with copper wire by conductive silver paste and then encapsulated by another PAA-PDMS film.

## 2.4. Characterizations

The morphology of PAA-PDMS elastomers were characterized using a scanning electron microscope (SEM, Phenom ProX, Phnomworld) with an acceleration voltage of 5 kV and optical microscope (OM, Eclipse LV100ND, Nikon). Attenuated total reflection Fourier transform infrared (ATR-FTIR) spectra were recorded using a Spectrum 400 (American, PerkinElmer). The ultraviolet-visible transmittance spectra were recorded with an UV-2600 spectrophotometer (Shimadzu). The tensile properties of PAA-PDMS elastomers were measured by a home-made test setup at a speed of 15 mm/min at room temperature. The electrical signals were performed in real-time by a digital source meter (Keithley 4200-SCS).

## 2.5. Tensile and electrical testing

All of the tensile tests, including tensile stress, tensile strain, tensile elongation, and loading-unloading tests were determined by the stress-strain curves. Tensile strength self-healing efficiency ( $\eta_\lambda$ ) is the ratio of the tensile strength of the pristine and healed devices. Tensile length self-healing efficiency ( $\eta_\rho$ ) is the ratio of the tensile elongation of the pristine and healed devices. The formulas are as follows:

$$\eta_\lambda = \frac{\lambda_H}{\lambda_P} \times 100\%,$$

$$\eta_\rho = \frac{\rho_H}{\rho_P} \times 100\%,$$

where  $\lambda_H$  and  $\lambda_P$  are the healed and initial tensile strength of devices, respectively.  $\rho_H$  and  $\rho_P$  are the healed and initial elongation at break of devices.

The resistance changes ( $\Delta R$ ) of PAA-PDMS/PEI-rGO strain sensors in different states were obtained by in real-time by a digital source meter (Keithley 4200-SCS). The relative resistance change of strain sensors is calculated on the basis of the current monitored:  $\Delta R/R_0 = (R - R_0)/R_0$ , where  $R$  and  $R_0$  are the resistance with and without applied strain, respectively. The averages and standard deviations were calculated from at least five samples for each sample.

## 3. Results and discussion

### 3.1. Fabrication of PAA-PDMS elastomers

Self-healable and self-adhesive PAA-PDMS elastomers were prepared by a convenient and efficient one-pot reaction. PAA has abundant carboxyl groups on its molecular chains, which facilitates its reaction by reactants containing functional groups (e.g, hydroxyl groups, carboxyl groups). In the preparation, first, the nitrogen with lone pair of electrons on the DCC attacks the carboxyl hydrogen of PAA. After the hydrogen is obtained, the carbon of DCC is positively charged. Then, the carboxyl oxygen after losing the hydrogen attacks the DCC intermediate carbon. Next, the lone pair electrons of nitrogen on the DMAP pyridine ring attacks carboxyl carbon. Meanwhile, another carboxyl group oxygen is removed from DCC to form DCU. Finally, N on the DMAP pyridine ring attacks hydroxyl hydrogen of PDMS-OH and obtains hydrogen. The hydroxyl group that loses hydrogen negatively attacks the carboxyl group carbon to form an ester group. Therefore, DCC and DMAP act as catalysts during preparing PAA-PDMS elastomers. Hence, the elastomers are formed by cross-linking PAA and hydroxyl-terminated PDMS (PDMS-OH) through covalent (i.e. ester groups) and dynamic bonding (i.e. hydrogen bonds). The covalent cross-linking between PAA and PDMS-OH is responsible for strengthening the mechanical properties of the PAA-PDMS elastomers. For PAA-PDMS elastomers, weak dynamic bonds should present as cross-linking sites so that elastomers could be break first upon damaging and reformed to self-heal. Additionally, PAA-PDMS elastomers cross-linked by dynamic hydrogen bonds tend to be soft and viscoelastic.

### 3.2. ATR-FTIR spectroscopy

To confirm the condensation reaction between PAA and PDMS-OH, the ATR-FTIR spectrum of PAA-PDMS elastomers films with PAA : PDMS-OH ratio of 3 : 1 was investigated (Fig. 1(a)), while the spectra of PAA and PAA & PDMS mixture were recorded as the control. The PAA, PAA & PDMS and PAA-PDMS films were prepared as same thickness of 0.5 mm films for testing ATR-FTIR spectroscopy. In particular, compared with PAA-PDMS, there is no DCC and DMAP catalyst in PAA & PDMS material, which indicates that there is no reaction between PAA and PDMS-OH under normal conditions. For the PAA and PAA & PDMS, an absorption band at

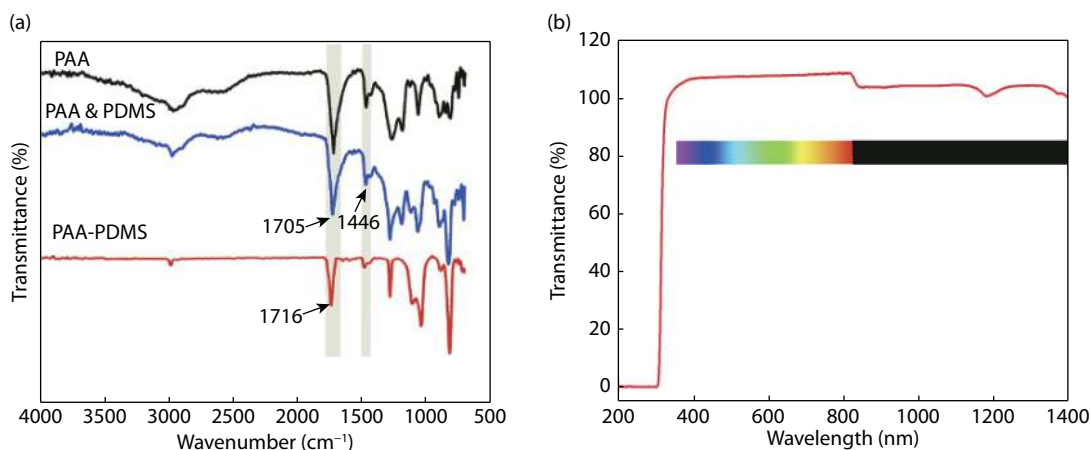


Fig. 1. (Color online) (a) ATR-FTIR and (b) UV spectra of neat PAA, PAA & PDMS and PAA-PDMS materials.

Table 1. Mechanical properties of elastomer with different ratios of PAA and PDMS-OH.

Sample	PAA:PDMS-OH (wt.%)	Breaking strength (MPa)	Breaking elongation (%)
F-1-1	1 : 1	0.4832	76.7
F-2-1	2 : 1	0.4426	91.3
F-3-1	3 : 1	0.3829	94.5
F-5-1	5 : 1	0.3749	146.4
F-10-1	10 : 1	0.3365	148.6

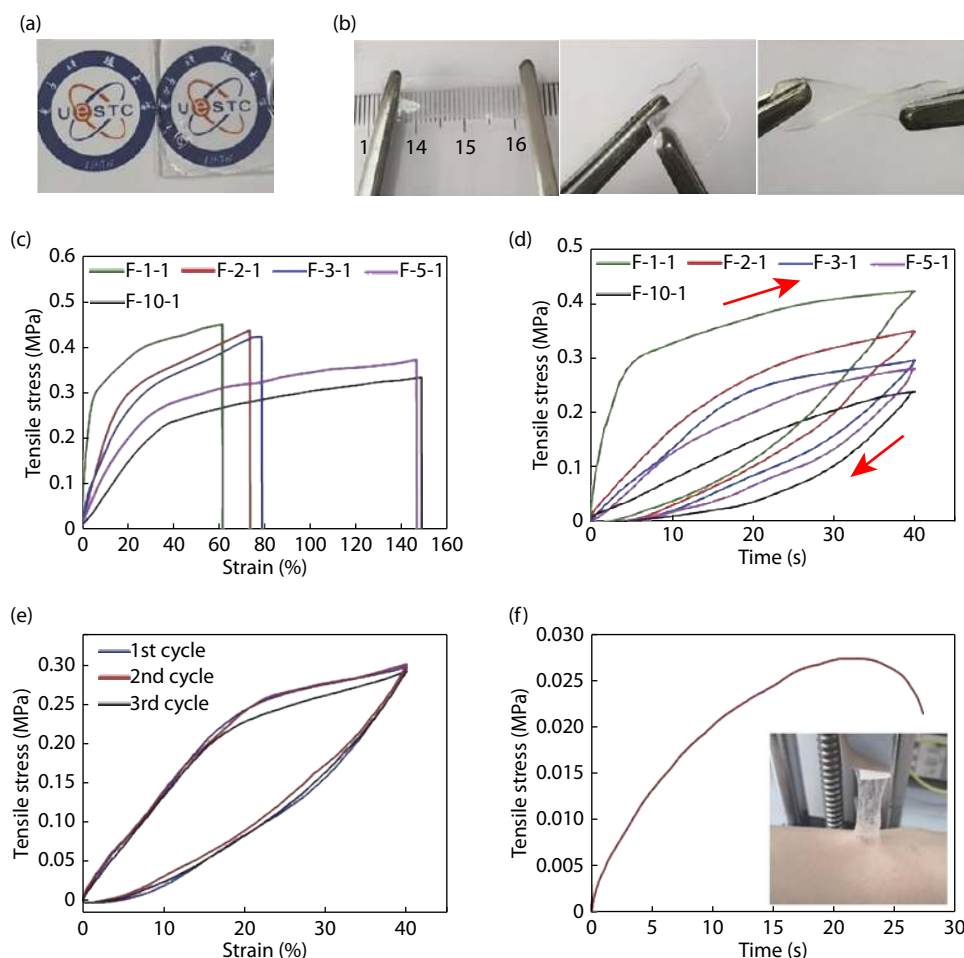


Fig. 2. (Color online) Physical properties of PAA-PDMS elastomers. (a) Photographic image of the transparent PAA-PDMS elastomer film. (b) Photographic images of PAA-PDMS films under stretching, bending, and twisting. (c) Typical tensile stress-strain curves of films with various weight ratios between PAA and PDMS-OH (F-1-1, F-2-1, F-3-1, F-5-1, and F-10-1). (d) and (e) Tensile stress-strain curves of PAA-PDMS films within 40% strain under loading-unloading cycle. (f) Tensile stress between PAA-PDMS elastomer and skin. Insert photo shows adhesion strength test of the PAA-PDMS elastomer on skin.

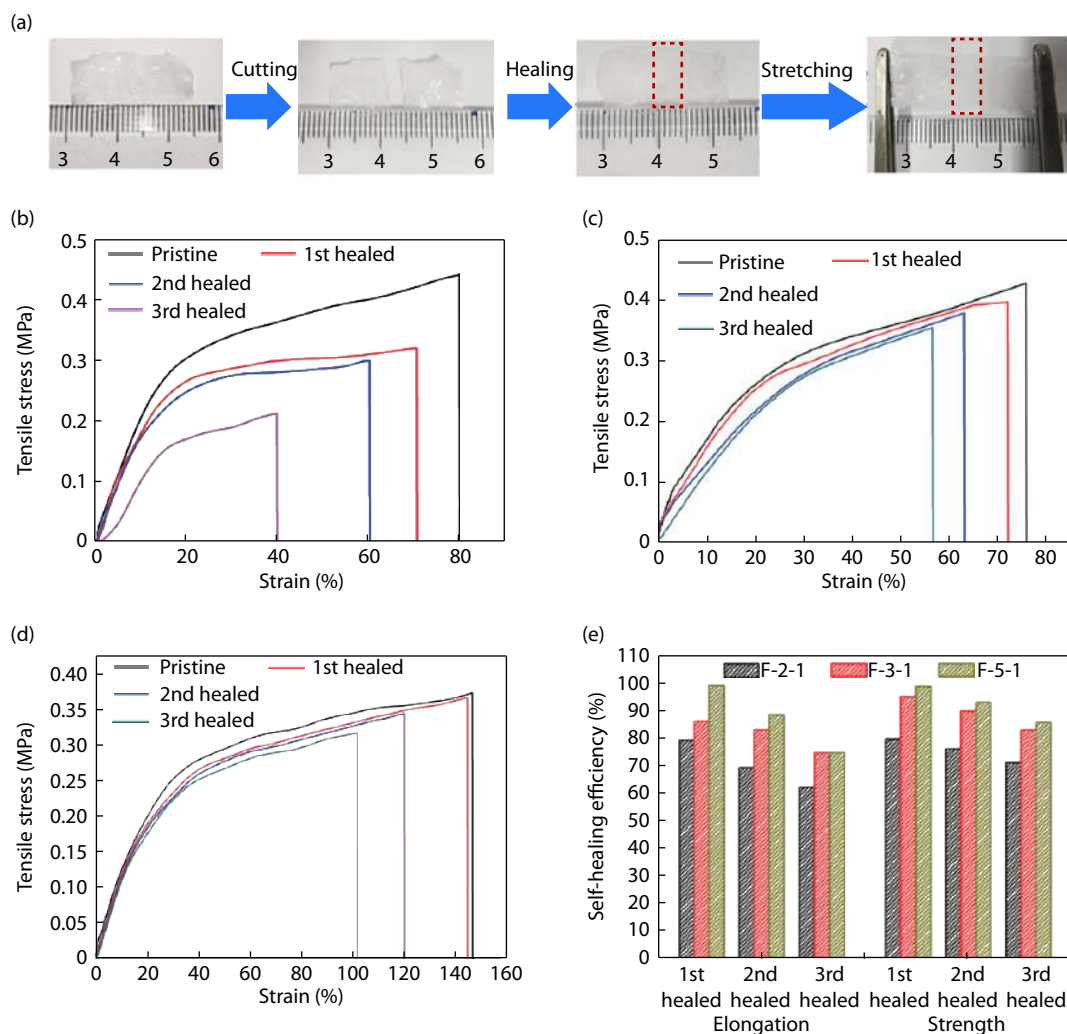


Fig. 3. (Color online) Self-healing properties of PAA-PDMS elastomers. (a) Photographic images of self-healing process of F-3-1 film, the healed film is mechanically stable under stretching. Typical tensile stress-strain curves for (b) F-2-1, (c) F-3-1 and (d) F-5-1 film during three cutting-healing cycles. (e) Self-healing efficiencies of PAA-PDMS elastomer films of F-2-1, F-3-1, and F-5-1 during three cutting-healing cycles.

1705  $\text{cm}^{-1}$  was observed, which belongs to the stretching vibration of C=O in  $-\text{COOH}$ . For the PAA-PDMS elastomers, a red shift of the stretching vibration of C=O to 1716  $\text{cm}^{-1}$  was observed, indicating the formation of ester groups. This confirmed the crosslinking between PAA and PDMS-OH.

### 3.3. Mechanical properties of PAA-PDMS elastomers

The elastomer films ( $25 \times 25 \times 0.5 \text{ mm}^3$ ) were prepared by various weight ratios of PAA and PDMS-OH (Table 1), which are transparent with outstanding optical transmittance of  $\sim 100\%$  in full visible light region (Figs. 1(b) and 2(a)). The transmittance greater than 100% is mainly due to the half-wave loss of the film and the inter-interface emission, which is consistent with other work have been reported<sup>[38, 39]</sup>. The PAA-PDMS films are mechanically stable and they can be bent, stretched, and twisted without breaking (Fig. 2(b)). Additionally, F-1-1, F-2-1, F-3-1, F-5-1 and F-10-1 samples are defined as 1 : 1, 2 : 1, 3 : 1, 5 : 1 and 10 : 1 weight ratio of PAA and PDMS-OH to obtain elastomer film, respectively (Table 1). The tensile performances of the elastomer films were quantitatively investigated by stress-strain curves (Fig. 2(c)). With the increase of PAA ratios in the films, the fracture stress decreased from 0.48 to 0.34 MPa, while the elongation at break increased from 76.7% to 148.6% (Table 1). The results are in-

duced by the increased contents of dynamic hydrogen bonds, which further enhance movement of polymer chains. Hydrogen bonds in the PAA-PDMS elastomers increase the dynamicity and mobility, but decrease the mechanical strength of the films simultaneously.

The elasticity of PAA-PDMS films was investigated by cyclic tensile tests, which indicates hydrogen bonds recovery in the cross-linked networks (Fig. 2(d)). Typical hysteresis and residual strain are observed for all the PAA-PDMS elastomer films stretched to a strain of 40%. After relaxing the external strength, the films shrink back to origin length. The film of F-10-1 shows a much lower tensile strength compared to the other films (F-1-1, F-2-1, F-3-1, and F-5-1) due to the higher content of dynamic hydrogen bonds. With the increased PAA contents, the hysteresis of elastomer films during loading-unloading cycles increase. The three stretching-releasing curves are highly coincident for F-3-1 within a 40% applied strain, indicating the hydrogen bonds recovery in the cross-linked networks (Fig. 2(e)). Combining with the above features, the PAA-PDMS elastomers have the potential to be applied as substrates or packaging for stretchable sensors for physical deformations detecting. Moreover, the mechanical properties (e.g. strength, elasticity) of these elastomers can be tuned by varying the weight ratios between PAA and PDMS-OH.

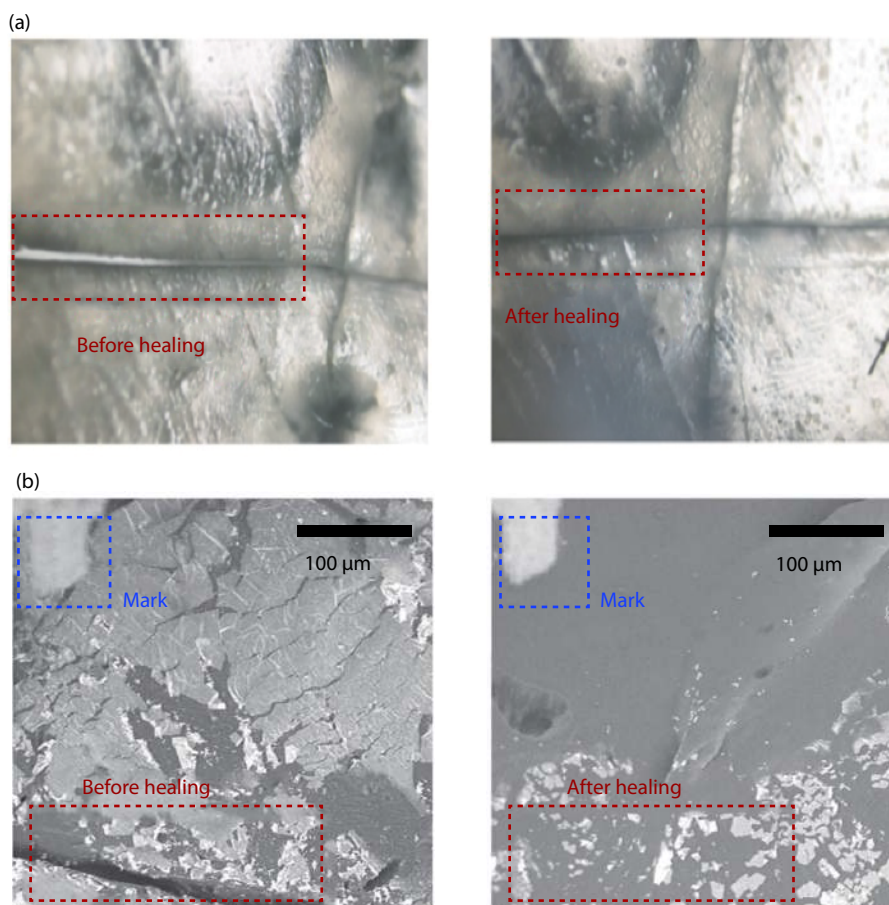


Fig. 4. (Color online) OM and SEM images of healed PAA-PDMS elastomer. (a) OM images of the self-healing process of F-3-1 without any external stimulus. (b) SEM images of the self-healing process (surface cut) of F-3-1 under vapor treating, the process is finished in ~3 min.

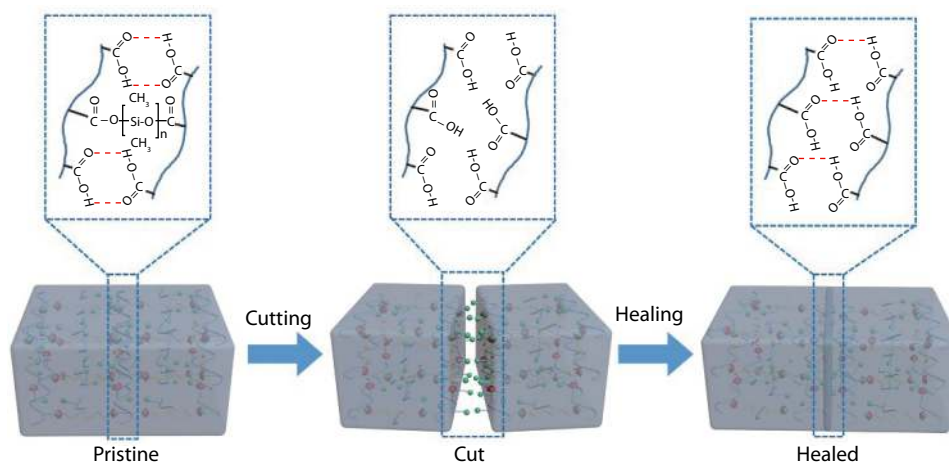


Fig. 5. (Color online) Schematic illustrations of the self-healing process of PAA-PDMS elastomers.

Additionally, PAA shows great potential in the fabrication of wearable sensors with excellent biocompatible tissue adhesiveness<sup>[40–43]</sup>. Due to the abundant carboxyl groups on the surface, the PAA-PDMS elastomers are biocompatible and self-adhesive to skin (Fig. 2(f) and Movie S1). A strong adhesion strength, as high as ~0.028 MPa, was observed between PAA-PDMS elastomer and skin. The elastic modulus of the PAA-PDMS elastomers is comparable with that of human skin (10–500 kPa), providing the PAA-PDMS elastomers with a good level of comfort with the human body<sup>[44]</sup>. Furthermore, when applied as wearable sensors, the self-adhesiveness en-

ables the elastomer to be directly attached onto human skin without requiring any additional adhesive tapes, which facilitates detecting accuracy and convenience during practical monitoring.

### 3.4. Self-healing properties of PAA-PDMS elastomers

The PAA-PDMS elastomers with reversible hydrogen bonds are expected to be self-healable. A film of F-3-1 was cut by a razor blade into two halves, and then gently brought back to contact immediately without any applied stress. After healing for 10 s, the two separate pieces can self-heal automatically under room temperature, which is faster than the oth-

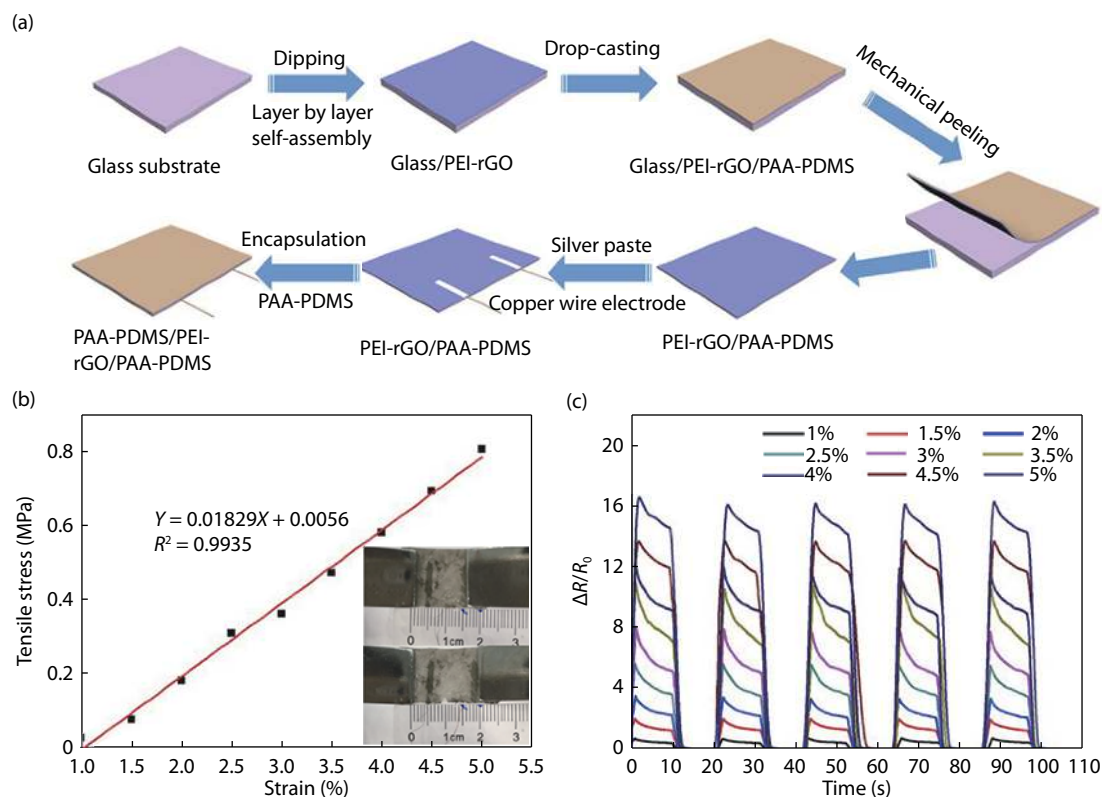


Fig. 6. (Color online) The fabrication, electrical and mechanical properties of PAA-PDMS/PEI-rGO sensors. (a) Schematic illustration of preparing PAA-PDMS/PEI-rGO sensors. (b) Variations of tensile performance of the PAA-PDMS/PEI-rGO sensor vs. applied strain. (c) The response of the self-healing strain sensors under various applied tensile strains after 500 stretching/releasing cycles under 3% applied strain.

er studies that require additional external stimuli (i.e. light<sup>[45]</sup>, heat<sup>[46]</sup>) or a healing agent. In Fig. 3(a) it can be seen that the healed films are highly flexible and stretchable, even after several cutting-healing cycles.

The recyclability of PAA-PDMS films were investigated by cutting and healing for three cycles at the same position. Typical tensile stress-strain curves were measured for healed F-2-1, healed F-3-1, and healed F-5-1 (Figs. 3(b)–3(d)). All of the elastomer films show good recovery of mechanical properties after three cutting-healing cycles. Compared with F-3-1 and F-5-1, which can self-heal quickly under room temperature, the self-healing process of F-2-1 is slow and needed to be triggered by water vapor for 2–3 min. The self-healing efficiencies of F-2-1, F-3-1, and F-5-1 after each cutting-healing cycle are summarized in Fig. 3(e). F-2-1 film heals ~95.9% and ~77% of its original elongation and strength at break after the first cutting-healing cycle, which decrease to ~54.1% and ~51.0% after the third cutting-healing cycle. With the increase of PAA contents, the elastomer films show higher healing efficiencies due to the increased content of dynamic hydrogen bonds, which help to promote the self-healing process. The films of F-3-1 and F-5-1 recover ~74.6%, 74.7% elongation and ~82.7%, 85.5% strength at break after the third cutting-healing cycle.

The self-healing process of F-3-1 was monitored by optical microscope (OM) and scanning electron microscope (SEM). Two separated pieces of F-3-1 after complete cutting were contacted under room temperature without any external stimulus. The self-healing process was recorded by an OM (Fig. 4(a) and Movie S2). The film was almost completely mended to a uniform material except a scar left on surface. This could be

one of the reasons for the incomplete recovery of mechanical properties after healing. The surface cut can be completely healed after treating by water or water vapor for ~3 min, due to the increased mobility of polymer chains in humid environment (Fig. 4(b)). The PAA-PDMS elastomers are able to self-heal the surface cut and therefore have the potential to be applied in fabricating optical devices, including lens and packaging layers of optical sensors.

According to the results, the corresponding illustration of the self-healing process of PAA-PDMS elastomers is as follows (Fig. 5). The covalent ester groups and dynamic hydrogen bonds were broken simultaneously during cutting of the PAA-PDMS elastomers. Subsequently, after contacting the two separated pieces, hydrogen bonds between carboxyl groups on PAA were reformed and induced the self-healing process. However, with more cutting-healing cycles, less covalent bonds are left<sup>[40]</sup>, which induces decrease of the mechanical properties and self-healing efficiency.

### 3.5. PAA-PDMS/PEI-rGO sensors

The PAA-PDMS elastomers with excellent mechanical properties, fast self-healing ability and comfortable self-adhesiveness to skin have the potential to be applied in strain sensors. As PAA content increases, the elastomer films show increased self-healing efficiencies and decreased mechanical properties. Therefore, taking account of both factors, the elastomer with PAA : PDMS-OH ratio of 3 : 1 was used to fabricate the packaging-layer of strain sensors.

A novel PAA-PDMS/PEI-rGO strain sensor was prepared by assembling PAA-PDMS elastomers and conductive PEI-rGO hierarchical nanocomposite films according to our previous study (Fig. 6(a))<sup>[37]</sup>. The hierarchical PEI-rGO core-layers and

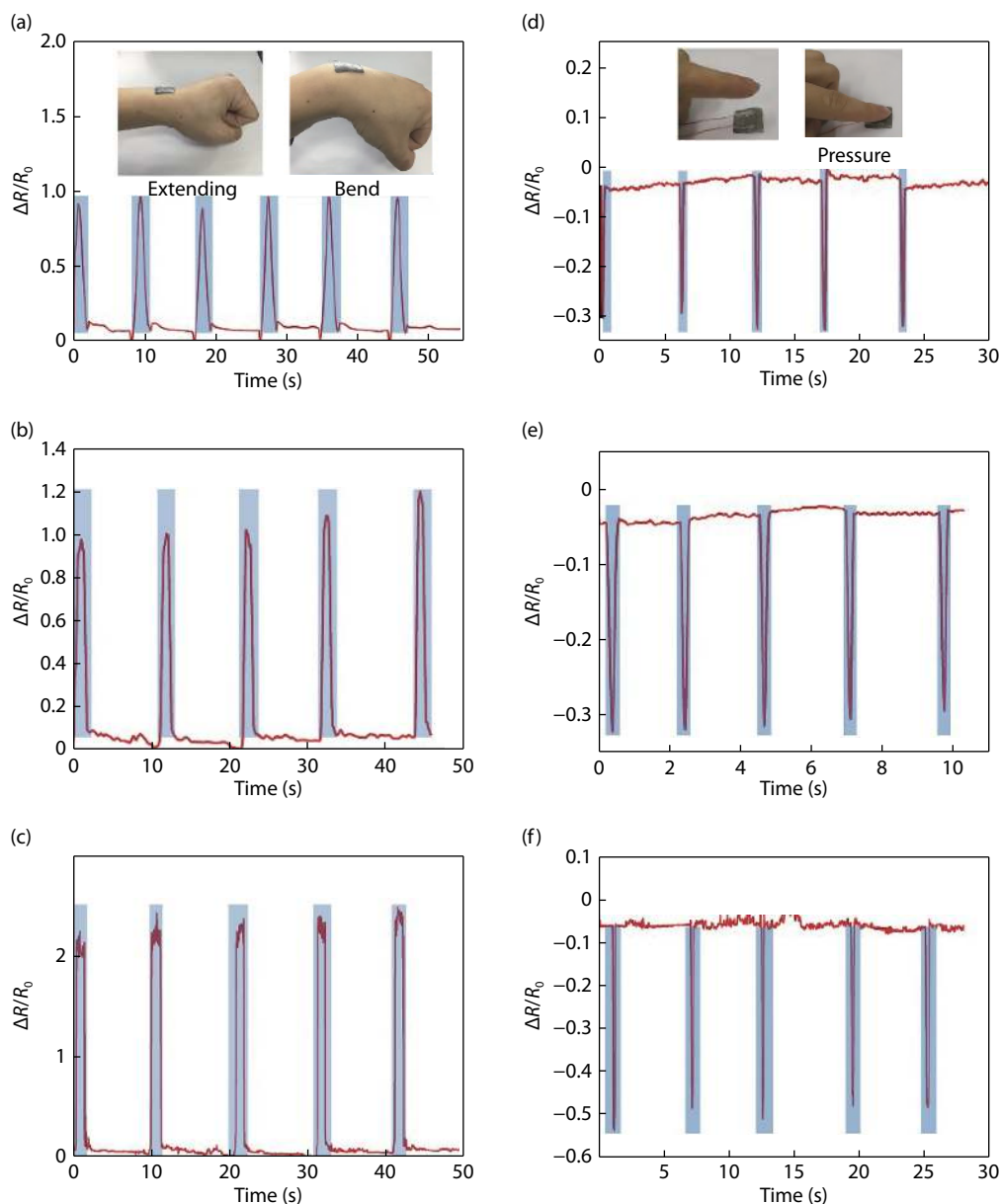


Fig. 7. (Color online) Application of PAA-PDMS/PEI-rGO strain sensors: the corresponding response to the (a–c) wrist and (d–f) press of the pristine, surface cut healed and complete cut healed strain sensors.

PAA-PDMS shell-layers enable the strain sensors with superior sensitivity, self-healing, self-adhesiveness, and biocompatibility, which can be directly worn on the skin and applied in detecting physical deformations.

During practical applications, the tensile stress and response of PAA-PDMS/PEI-rGO sensors within 5% strain were investigated. The tensile stress is well-linear to the applied strain, indicating the potential of the PAA-PDMS/PEI-rGO sensors in detecting slight motions (Fig. 6(b)). The strain sensors are remarkably stable, repeatable, and durable during stretching-releasing testing. Applied strains varying from 1% to 5% can be reliably monitored by the PAA-PDMS/PEI-rGO sensors after 500 stretching-releasing cycles within 3% applied strain (Fig. 6(c)).

The PAA-PDMS/PEI-rGO sensors were directly adhered on the wrist without requiring any external additional adhesive tapes to monitor body motions (Fig. 7(a)). Additionally, no irritation is induced to the skin by the PAA-PDMS/PEI-rGO sensors in  $\sim 2$  h. When the wrist was bent downwards, the

sensor was stretched with its resistance increased abruptly. The resistance gradually restored to the original value after the forefinger returned straight, which is consistent with the mechanism of strain sensors<sup>[26, 37]</sup>. During the multiple bending-unbending cycles of the wrist, the varying resistance curve shows a regular and repeatable shape, indicating that the response of the PAA-PDMS/PEI-rGO sensors is reliable and stable.

The PAA-PDMS/PEI-rGO sensors can self-heal a shallow scratch on the surface, which are able to be reused for monitoring body motions. After shallowly cutting on the surface, the self-healing process of the strain sensors is accomplished in  $\sim 10$  s at room temperature. The healed sensors detect the motion of wrist and press, and output stable and reproducible signals (Figs. 7(b) and 7(e)). The corresponding relative resistance responses of the healed sensors were consistent with those of the pristine sensors. Additionally, even after completely cutting, the PAA-PDMS/PEI-rGO sensors can still be self-healed and are able to detect wrist bending and

pressure (Figs. 7(c) and 7(f)). Stable and reproducible waveform signals were obtained, and it is believed that the movement and fusion of PAA-PDMS networks induces the connection of PEI-rGO layers during the self-healing process, which partially heals the strain sensors. However, the resistance change ( $\Delta R$ ) of the healed sensors is much higher than the pristine sensors, which is attributed to the lack of self-healing ability of PEI-rGO conducting layers.

#### 4. Conclusion

In summary, we successfully fabricated a novel transparent, biocompatible, self-adhesive, and self-healing elastomer by cross-linking PAA and PDMS-OH through a convenient and efficient one-pot reaction. The PAA-PDMS elastomers are mechanically stable and elastic. The abundant carboxyl groups on surface facilitate the PAA-PDMS elastomers with robust self-adhesiveness. The dynamic nature of PAA-PDMS elastomers on the basis of the hydrogen bonds manifests the elastomers with fast (within 10 s) and efficient (~98%) self-healing ability under room temperature without any external stimulus. Strain sensors were fabricated by assembling the PAA-PDMS packaging layers and PEI-rGO conducting layers. The PAA-PDMS/PEI-rGO strain sensors exhibit stable and reliable response to physical deformations, which can be further worn on the skin to monitor the body's motions. The strain sensors can completely self-heal a shallow cut on the surface and they can reliably detect slight body motions. However, further improving self-healing ability is necessary for the PAA-PDMS/PEI-rGO sensors, especially for the case of complete cutting. The PEI-rGO layers without self-healing ability decrease the stability and reliability of the sensors after healing. This challenge might be addressed in the future by fabricating self-healable conducting layers<sup>[9, 28]</sup>.

#### Acknowledgements

This work is supported by the National Science Funds for Excellent Young Scholars of China (Grant No. 61822106), National Science Funds for Creative Research Groups of China (Grant No. 61421002), Natural Science Foundation of China (Grant No. 61671115) and Opening Project of State Key Laboratory of Polymer Materials Engineering (Sichuan University) (Grant No. sklpm2018-4-28).

#### References

- [1] Hager M D, P Greil P, C Leyens C, et al. Self-healing materials. *Adv Mater*, 2010, 22, 5424
- [2] Wool R P. Self-healing materials: a review. *Soft Matter*, 2008, 4(3), 400
- [3] White S R, N Sottos N, P Geubelle P, et al. Autonomic healing of polymer composites. *Nature*, 2001, 409(6822), 794
- [4] Cho S H, White S R, Braun P V. Self-healing polymer coatings. *Adv Mater*, 2009, 21(6), 645
- [5] Zwaag S. Self-healing materials: An alternative approach to 20 centuries of materials science. The Netherlands: Springer Science Business Media BV, 2008, 30
- [6] Han Y, Wu X, Zhang X, et al. Self-healing, highly sensitive electronic sensors enabled by metal-ligand coordination and hierarchical structure design. *ACS Appl Mater Interfaces*, 2017, 9(23), 20106
- [7] Yamada T, Hayamizu Y, Yamamoto Y, et al. A stretchable carbon nanotube strain sensor for human-motion detection. *Nanotech*, 2011, 6(5), 296
- [8] Yang Y, Zhu B, Yin D, et al. Flexible self-healing nanocomposites for recoverable motion sensor. *Nano Energy*, 2015, 17, 1
- [9] Hu Y, Zhao T, Zhu P, et al. A low-cost, printable, and stretchable strain sensor based on highly conductive elastic composites with tunable sensitivity for human motion monitoring. *Nano Res*, 2018, 11(4), 1938
- [10] Liao M, Wan P, Wen J, et al. Wearable, healable, and adhesive epidermal sensors assembled from mussel-inspired conductive hybrid hydrogel framework. *Adv Funct Mater*, 2017, 27(48), 1703852
- [11] Chen P, Li Q, Grindy S, et al. White-light-emitting lanthanide metallogels with tunable luminescence and reversible stimuli-responsive properties. *Chem Soc*, 2015, 137(36), 11590
- [12] Wang C, Wu H, Chen Z, et al. Self-healing chemistry enables the stable operation of silicon microparticle anodes for high-energy lithium-ion batteries. *Nat Chem*, 2013, 5(12), 1042
- [13] Jin H, Huynh T P, Haick H. Self-healable sensors based nanoparticles for detecting physiological markers via skin and breath: toward disease prevention via wearable devices. *Nano Lett*, 2016, 16(7), 4194
- [14] Pantelopoulou A, Bourbakis N G. A survey on wearable sensor-based systems for health monitoring and prognosis. *IEEE Trans Syst Man Cy C*, 2010, 40(1), 1
- [15] Wang D Y, Tao L Q, Y Liu Y, et al. High performance flexible strain sensor based on self-locked overlapping graphene sheets. *Nanoscale*, 2016, 8(48), 20090
- [16] Pang C, Lee C, Suh K Y. Recent advances in flexible sensors for wearable and implantable devices. *J Appl Polym Sci*, 2013, 130(3), 1429
- [17] Choi S, Lee H, Ghaffari R, et al. Recent advances in flexible and stretchable bio-electronic devices integrated with nanomaterials. *Adv Mater*, 2016, 28(22), 4203
- [18] Chen D, Wang D, Yang Y, et al. Self-healing materials for next-generation energy harvesting and storage devices. *Adv Energy Mater*, 2017, 7(23), 1700890
- [19] Gao N, Fang X. Synthesis and development of graphene-inorganic semiconductor nanocomposites. *Chem Rev*, 2015, 115(16), 8294
- [20] Ning Y, Zhang Z, Teng F, et al. Novel transparent and self-powered UV photodetector based on crossed ZnO nanofiber array homojunction. *Small*, 2018, 14(13), 1703754
- [21] Darabi M A, A Khosrozadeh A, R Mbeleck R, et al. Skin-inspired multifunctional autonomic-intrinsic conductive self-healing hydrogels with pressure sensitivity, stretchability, and 3D printability. *Adv Mater*, 2017, 29(31), 1700533
- [22] Li J, Geng L, Wang G, et al. Self-healable gels for use in wearable devices. *Chem Mater*, 2017, 29(21), 8932
- [23] Cai G, Wang J, Qian K, et al. Extremely stretchable strain sensors based on conductive self-healing dynamic cross-links hydrogels for human-motion detection. *Adv Sci*, 2017, 4(2), 1600190
- [24] Liu Y J, Cao W T, Ma M G, et al. Ultrasensitive wearable soft strain sensors of conductive, self-healing, and elastic hydrogels with synergistic "soft and hard" hybrid networks. *ACS Appl Mater Interfaces*, 2017, 9(30), 25559
- [25] Liu S, Zheng R, Chen S, et al. A compliant, self-adhesive and self-healing wearable hydrogel as epidermal strain sensor. *J Mater Chem C*, 2018, 6(15), 4183
- [26] Liu X, Lu C, Wu X, et al. Self-healing strain sensors based on nanostructured supramolecular conductive elastomers. *J Mater Chem A*, 2017, 5(20), 9824
- [27] Keller M W, White S R, Sottos N R. A self-healing poly (dimethyl siloxane) elastomer. *Adv Funct Mater*, 2007, 17(14), 2399
- [28] Zhang D D, Ruan Y B, Zhang B Q, et al. A self-healing PDMS elastomer based on acylhydrazone groups and the role of hydrogen bonds. *Polymer*, 2017, 120, 189



- [29] Zhang A, Yang L, Lin Y, et al. Self-healing supramolecular elastomers based on the multi-hydrogen bonding of low-molecular polydimethylsiloxanes: Synthesis and characterization. *J Appl Polym Sci*, 2013, 129(5), 2435
- [30] Zhao J, Xu R, Luo G, et al. A self-healing, re-moldable and biocompatible crosslinked polysiloxane elastomer. *J Mater Chem B*, 2016, 4(5), 982
- [31] Zhang B, Zhang P, Zhang H, et al. A transparent, highly stretchable, autonomous self-healing poly(dimethyl siloxane) elastomer. *Macromol Rapid Commun*, 2017, 38(15), 1700110
- [32] Mei J F, Jia X Y, Lai J C, et al. A highly stretchable and autonomous self-healing polymer based on combination of pt-pt and  $\pi$ - $\pi$  interactions. *Macromol Rapid Comm*, 2016, 37(20), 1667
- [33] Jia X Y, Mei J F, Lai J C, et al. A self-healing PDMS polymer with solvatochromic properties. *Chem Commun*, 2015, 51(43), 8928
- [34] Jia X Y, Mei J F, Lai J C, et al. A highly stretchable polymer that can be thermally healed at mild temperature. *Macromol Rapid Commun*, 2016, 37(12), 952
- [35] Rao Y L, Chortos A, Pfattner R, et al. Stretchable self-healing polymeric dielectrics cross-linked through metal-ligand coordination. *J Am Chem Soc*, 2016, 138(18), 6020
- [36] Cao J, Zhang X, Lu C, et al. Self-healing sensors based on dual non-covalent network elastomer for human motion monitoring. *Macromol Rapid Commun*, 2017, 38(23), 1700406
- [37] Ye X, Yuan Z, Tai H, et al. A wearable and highly sensitive strain sensor based on a polyethylenimine-rGO layered nanocomposite thin film. *J Mater Chem C*, 2017, 5(31), 7746
- [38] Shobhana E. X-Ray diffraction and UV-visible studies of PMMA thin films. *Int J Modern Eng Res*, 2012, 2(3), 1092
- [39] Wang T, Isimjan T T, Chen J, et al. Transparent nanostructured coatings with UV-shielding and superhydrophobicity properties. *Nanotechnology*, 2011, 22(26), 265708
- [40] De Giglio E, Cometa S, Cioffi N, et al. Analytical investigations of poly (acrylic acid) coatings electrodeposited on titanium-based implants: a versatile approach to biocompatibility enhancement. *Anal Bioanal Chem*, 2007, 389(7/8), 2055
- [41] Yu H, Fu G, He B. Preparation and adsorption properties of PAA-grafted cellulose adsorbent for low-density lipoprotein from human plasma. *Cellulose*, 2006, 14(2), 99
- [42] Dai J, Bao Z, Sun L, et al. High-capacity binding of proteins by poly (acrylic acid) brushes and their derivatives. *Langmuir*, 2006, 22(9), 4274
- [43] Drotlef D M, Amjadi M, Yunusa M, et al. Bioinspired composite microfibers for skin adhesion and signal amplification of wearable sensors. *Adv Mater*, 2017, 29(28), 1701353
- [44] Liu Y, Pharr M, Salvatore G A. Lab-on-skin: a review of flexible and stretchable electronics for wearable health monitoring. *ACS Nano*, 2017, 11(10), 9614
- [45] Song Y K, Jo Y H, Lim Y J, et al. Sunlight-induced self-healing of a microcapsule-type protective coating. *ACS Appl Mater Interfaces*, 2013, 5(4), 1378
- [46] Mangun C L, Mader A C, Sottos N R, et al. Self-healing of a high temperature cured epoxy using poly (dimethylsiloxane) chemistry. *Polymer*, 2010, 51(18), 4063